Partially asymmetric exclusion processes with sitewise disorder

Róbert Juhász*
Fachrichtung Theoretische Physik, Universität des Saarlandes, D-66041 Saarbrücken, Germany
and Research Institute for Solid State Physics and Optics, H-1525 Budapest, P.O. Box 49, Hungary

Ludger Santen†
Fachrichtung Theoretische Physik, Universität des Saarlandes, D-66041 Saarbrücken, Germany

Ferenc Iglói‡
Research Institute for Solid State Physics Optics, H-1525 Budapest P.O. Box 49, Hungary
and Institute of Theoretical Physics, Szeged University, H-6720 Szeged, Hungary
(Received 14 July 2006; published 4 December 2006)

We study the stationary properties as well as the nonstationary dynamics of the one-dimensional partially asymmetric exclusion process with position-dependent random hop rates. Relating the hop rates to an energy landscape the stationary current J is determined by the largest barrier in a finite system of L sites and the corresponding waiting time $\tau \sim J^{-1}$ is related to the waiting time of a single random walker, τ_{rw}, as $\tau \sim \tau_{rw}^{1/2}$. The current is found to vanish as $J \sim L^{-z/2}$, where z is the dynamical exponent of the biased single-particle Sinai walk. Typical stationary states are phase separated: At the largest barrier almost all particles queue at one side and almost all holes are at the other side. The high-density (low-density) region is divided into $\sim L^{1/2}$ connected parts of particles (holes) which are separated by islands of holes (particles) located at the subleading barriers (valleys). We also study nonstationary processes of the system, like coarsening and invasion. Finally we discuss some related models, where particles of larger size or multiple occupation of lattice sites is considered.

DOI: 10.1103/PhysRevE.74.061101 PACS number(s): 05.60.−k, 05.40.−a, 05.70.Ln, 64.60.−i

I. INTRODUCTION

The stochastic dynamics of self-driven particles on one-dimensional lattices is one of the key problems of nonequilibrium physics [1,2]. Models of this kind have been used in order to describe such problems as, e.g., highway traffic [3] or the dynamics of motor proteins along actin filaments or microtubuli [4]. These two examples have in common that the directed particle motion against dissipative forces is maintained by the steady input of energy, a feature that leads to generic nonequilibrium behavior of the system. The drift of the particles also leads to a strong sensitivity to spatial inhomogeneities; e.g., in contrast to equilibrium systems, even a single local defect may lead to bulk effects such as, e.g., separation into macroscopic low- and high-density domains [5]. Moreover disorder of any type may also strongly influence the transport capacities of the system [6–9]. This is in particular true for the case of strong disorder—i.e., realizations of the disorder where the local direction of the bias is nonuniform [10–12,19]. The prototype of this kind of stochastic motion is the Sinai walk, which has been studied to a great extent [13]. The stochastic motion of a Sinai walker is characterized by large velocity fluctuations. The origin of these fluctuations is most easily understood if one translates the local hop rates into energy differences; i.e., a forward bias corresponds to a negative slope of the corresponding energy landscape and vice versa. Obviously, the energy landscape is not flat in the case of strong disorder, but characterized by barriers of different heights. The time a walker spends in front of such a barrier increases exponentially with the height of the barrier, and therefore the largest barriers determine the behavior of the system.

There exists a large class of both quantum and stochastic models where the quenched disorder dominates the fluctuations in the system and where a connection to the Sinai walk can be made [14]. In this respect one can mention random quantum spin chains [15,16] or reaction diffusion models with quenched disorder [17]. Besides a number of experimental setups have been identified, where this model properly describes the particle dynamics—e.g., the translocation of an RNA strand through a pore [18] or the motion of molecular motors on microtubules [4].

While most of the models refer to the single-particle case, more recently the effect of strong disorder on driven-diffusive many-particle systems—i.e., the so-called asymmetric exclusion process with strong disorder—has been investigated [10–12,19–22]. It has been shown that the properties of the system largely depend on the way the disorder is implemented. In the case of particle disorder—i.e., for the case where the hop rates of the particles are quenched random variables [19]—the transport properties of the system are in close analogy to the single-particle system [11,12] both in the Griffiths phase—i.e., in the case of a tilted energy landscape—and at the critical point—i.e., for a vanishing drift velocity of the particles. This implies that the many-particle effects are most pronounced for quantities that are related to the arrangement of the particles. In the case of lattice disorder, however, the transport capacities of single-

*Electronic address: juhasz@lusi.uni-sb.de
†Electronic address: santen@lusi.uni-sb.de
‡Electronic address: igloi@szfki.hu

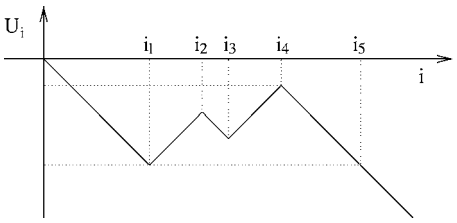

FIG. 1. Schematic energy landscape.

and many-particle systems are different [10,11], because the presence of many particles alters the effective heights of the energy barriers. A relation between the stationary current for particle disorder and for lattice disorder has been proposed in Ref. [11]. In the present work we elaborate on the properties of the distribution of the stationary current and show connections with extreme value statistics [23,24]. We also discuss the properties of the density profile as well as the consequences for the coarsening behavior. Some of the results obtained in this work may also be relevant for models which are closely related to the exclusion process, such as the Heisenberg chain [25] and the dimer evaporation and deposition process [26].

The article is organized as follows. The model is introduced in Sec. II, and the basic properties of the single-particle motion in the framework of the concept of trapping or waiting times are given in Sec. III. The stationary properties of the many-particle motion is presented for non zero average bias in Sec. IV and for zero average bias in Sec. V. Some related models are discussed in Sec. VI, and nonstationary phenomena are described in Sec. VII. In the final section we will summarize and discuss our results.

II. MODEL

We consider the partially asymmetric exclusion process (PASEP) with site-dependent hop rates on a one-dimensional lattice. Each lattice site i can either be empty—i.e., $\tau_i=0$—or occupied by a single particle, $\tau_i=1$.

The time evolution of the local configuration (τ_i,τ_{i+1}) is described by

$$(1,0)\rightarrow(0,1) \quad \text{with rate } p_i, \tag{1}$$

$$(0,1)\rightarrow(1,0) \quad \text{with rate } q_i; \tag{2}$$

i.e., particles are hopping in the positive direction (from i to site $i+1$) with rate p_i and in the negative direction (from site $i+1$ to site i) with rate q_i.

It is useful to relate the stochastic dynamics to an energy landscape by the relation

$$\frac{q_i}{p_i}=e^{-(U_i-U_{i+1})}, \tag{3}$$

where U_i is the energy assigned to site i (relative to a reference value $U_1=0$). A typical sample of this type of landscape is shown in Fig. 1. Links with forward bias $(q_i<p_i)$ correspond to descending links of the energy landscape while those with backward bias $(q_i>p_i)$ to ascending ones. It turns out that the large-scale behavior of the process is determined by the wandering properties of the energy landscape. The relation between energy landscape and system properties will be discussed in detail in the next section.

The hop rates are independent and identically distributed random variables taken from the distributions, $\rho(p)dp$ and $\pi(q)dq$, which will be specified later. We restrict ourselves to types of randomness where forward- and backward-directed links are present with finite probability; i.e., the easy direction of hopping is disordered as well. We define a control parameter as the average asymmetry between forward and backward rates as follows:

$$\Delta=\frac{[\ln p]_{\text{av}}-[\ln q]_{\text{av}}}{\text{var}[\ln p]+\text{var}[\ln q]}, \tag{4}$$

such that for $\Delta>0$ $(\Delta<0)$ the particles move on average to the right (left). Here and in the following, $[\cdots]_{\text{av}}$ denotes average over quenched disorder, whereas var(x) stands for the variance of x. Note that $\Delta\sim\lim_{L\rightarrow\infty}U_L/L$; thus, the control-parameter is proportional to the average slope of the potential landscape.

In most of the explicit calculations a binary disorder distribution is used,

$$\rho(p)=c\,\delta(p-1)+(1-c)\,\delta(p-r),$$

$$p_iq_i=r<1 \quad \text{for all } i, \tag{5}$$

where the control parameter is given by

$$\Delta=\frac{1-2c}{2c(1-c)\ln r}. \tag{6}$$

This implies that a biased motion to the right is realized for $1\leqslant c<1/2$.

Alternatively we also use a power-law distribution

$$\rho(p)=\frac{1}{D}p^{-1+1/D}, \quad 0<p\leqslant 1,$$

$$\pi(q)=\frac{q_0^{-1/D}}{D}q^{-1+1/D}, \quad 0<q\leqslant q_0, \tag{7}$$

where $D^2=\text{var}[\ln p]=\text{var}[\ln q]$ measures the strength of disorder and $\Delta=\ln q_0/(2D^2)$.

III. SINGLE-PARTICLE MOTION: THE CONCEPT OF TRAPPING TIMES

We wish to introduce in the next section a simple phenomenological approach to biased exclusion process, which is based on the dynamics of the corresponding single-particle problem, known as the Sinai walk [13,14]. This is a thoroughly studied system, and here we recapitulate some of its properties which are necessary to understand the many-particle problem: For a periodic chain of length L the stationary drift velocity v_0 for a given realization of disorder is given by [27]

$$\frac{1}{v_0} = \frac{1}{L}\sum_{i=1}^{L} \frac{1}{p_i \Pi_{i+1}} \left(1 - \prod_{i=1}^{L} \frac{q_i}{p_i} \right)^{-1}, \tag{8}$$

where

$$\Pi_{i+1} = \left(1 + \sum_{k=1}^{L-1} \prod_{j=1}^{k} \frac{q_{i+j-1}}{p_{i+j}} \right)^{-1} \tag{9}$$

is the persistence probability [28] at site $i+1$. This quantity measures the fraction of walks starting at site $i+1$ and pass the link $i,i+1$ first from the left—i.e., after a complete tour along the chain [29].

It is obvious that the regions where the particle spends long times are valleys of the energy landscape, which are followed by a large barrier. These sections of the energy landscape can be represented by Brownian excursions [30]—i.e., returning random walks staying in the upper half-plane [see the section (i_1,i_5) in Fig. 1].

It is obvious that one can define a (single-particle) trapping time for each barrier (Brownian excursion):

$$\tau_i = \frac{1}{p_i \Pi_{i+1}}, \tag{10}$$

which is the time needed to escape from that barrier and where i is the starting point of the corresponding excursion—i.e., the minimal energy site of the valley in front of the barrier (site i_1 in Fig. 1). It is important to notice that the trapping times take the form of a Kesten random variable [31]. Moreover, trapping times belonging to different barriers are practically independent, as the terms corresponding to links outside the barrier are exponentially small. It is known that in the large-L limit the probability distribution of such variables has an algebraic tail:

$$P(\tau) \sim \tau^{-1-1/z}, \tag{11}$$

where the exponent z is the positive root of the equation

$$\left[\left(\frac{q}{p} \right)^{1/z} \right]_{av} = 1. \tag{12}$$

Choosing the bimodal disorder as defined in Eq. (5) one obtains

$$z = \frac{\ln r}{\ln(c^{-1} - 1)}. \tag{13}$$

Now concerning the drift velocity of the random walker it is the inverse of the average trapping time for $z<1$. If, however, $z>1$, the average of the trapping time is divergent and the motion of a single particle is determined by the largest trapping time τ_m, the typical value of which follows from the relation [23] $\int_{\tau_m}^{\infty} P(\tau) d\tau L = O(1)$ and given by $\tau_m \sim L^z$.

The persistence probability and thus the trapping time at a given barrier is related to the potential landscape, and for large trapping times it is asymptotically given by

$$\tau_i \sim \sum_{k=1}^{L-1} \frac{1}{p_{i+k}} e^{U_{i+k}-U_i} \sim e^{\tilde{U}_i}, \tag{14}$$

which is well approximated by the largest term in the sum: $\tilde{U}_i = \max_k (U_{i+k} - U_i)$.

In this way the motion of the particle for $z>1$ is influenced only by the deep valleys and the corresponding large barriers, and ultimately its velocity is determined by passing the largest barrier in the system, since $\tau_m \sim e^{\tilde{U}_m}$ and $\tilde{U}_m = \max \tilde{U}_i$. The intimate relation between the mobility of the particle and structure of the energy landscape led to the idea of renormalizing the energy landscape [14,32]. By using the renormalization scheme and alternative approaches one obtains the same form of the trapping time distribution [33] as given in Eq. (11).

IV. MANY-PARTICLE MOTION

We now turn to the many-particle case; i.e., we put $N = O(L)$ particles on the lattice. First we consider a special form of disorder for which exact results can be derived. These are then generalized for more general form of disorder using phenomenological and scaling considerations.

A. Extreme binary disorder

Here we consider the bimodal disorder as defined in Eq. (5) where the landscape is represented by a random walk having a step of size $\ln r$ with probability $(1-c)$ and of size $-\ln r$ with probability (c). In the limit $c \ll 1$ the walk is strongly biased, having typically downwards steps and the rare upward steps are forming the barriers. If we also have $r \ll 1$, the large barriers are typically straight, since for a large energy scale the fluctuations are reduced [32]. The largest barrier consists of l_m upward steps and has a height of $\tilde{U}_m = l_m \ln r^{-1}$, and we have for the typical value $c^{l_m} L = 1$. It is easy to check that the trapping time for single-particle motion is $\tau_m \sim r^{l_m} \sim L^{z'}$ and the dynamical exponent $z' = \ln r / \ln c^{-1}$ corresponds to that in Eq. (13) in the given limit.

Also for many particles the largest barrier plays the dominant role and we analyze first the stationary current in a system having just one large barrier of length l_m. This problem corresponds to a PASEP with particle input and output against the direction of the bias. In the stationary state of this model, which is known exactly [34], the system is half-filled and there is a sharp front in the middle of the chain, which is the consequence of particle-hole symmetry. As a consequence particles (and holes) have to pass a half-filled barrier of effective height $\tilde{U}_m/2$. Consequently the effective trapping time is $\tilde{\tau}_m \sim \tau_m^{1/2}$ and the stationary current is given by

$$J \sim L^{-z/2}, \tag{15}$$

which goes to zero in the thermodynamic limit.

Now, if we consider the complete potential landscape, the basic features of the above considerations remain true, since the largest barrier governs the stationary dynamics of the system. In particular in the stationary state there is a sharp

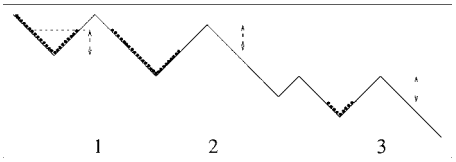

FIG. 2. Schematic form of the potential landscape for extreme disorder and the typical position of the particles. The high-density and low-density phases are separated at the middle of the largest barrier (2); the arrow indicates the height $U_m/2$. Deep valleys in the low-density phase are filled until the effective barrier is $U_m/2$ (3) and high barriers in the high-density phase are vacant above a level of $U_m/2$ (1); see text.

front located at the middle of the largest barrier. Thus, due to particle-hole symmetry, the largest barrier is half-filled and the stationary current is related to the largest effective trapping time and given by Eq. (15). The subleading barriers lead to a substructure both in the high-density and in the low-density phases, which can be related to each other by using the particle-hole symmetry. In the low-density region it is easy to see that small barriers with $\tilde{U}_i < \tilde{U}_m/2$ are completely empty, since they do not cause sufficient resistivity for the current. Only sufficiently large barriers with $\tilde{U}_i > \tilde{U}_m/2$ are able to slow down the particle and cause jams. These barriers will be filled up to the level $\tilde{U}_i - \tilde{U}_m/2$ as a consequence of the conservation of the stationary current. The typical number of occupied barriers in the low-density phase is given by $c^{l_m/2}L \sim L^{1/2}$. In the high-density phase, due to particle-hole symmetry, holes are accumulated only in such subleading barriers for which $\tilde{U}_i > \tilde{U}_m/2$. The number of holes in such a barrier scales as $\tilde{U}_i - \tilde{U}_m/2$, and the typical number of occupied barriers is $O(L^{1/2})$.

B. General form of disorder

Next we extend our discussion to general form of disorder, when it may be still assumed that there is a sharp front separating the high-density and low-density regions. If this is the case, the front is located at a position where the escape rate of particles and the escape rates of holes which leave the front to the left through the high-density region are equal, which is a necessary condition for the localization of the front. As in the extreme disorder case, the front is located in the middle of the largest barrier. The potential landscape compared with that for extreme disorder in Fig. 2 is modified in such a way that instead of long straight lines the barriers and valleys are made by Brownian excursions.

1. Distribution of the current

The typical value of the stationary current follows from the same reasoning as in Sec. IV A: it is given by the square root of the trapping time of a single walker at the largest barrier. Furthermore, the trapping time distribution follows an asymptotically algebraic distribution given by (11).

Therefore for a given system we have to find the maximum out of $O(L)$ algebraically distributed random variables, a problem which is thoroughly studied in the mathematical literature (see, e.g., [23]) and has demonstrated to work for strong Griffiths singularities in disordered systems [24]. For our case it follows that the current is described by the well-known Fréchet distribution given by

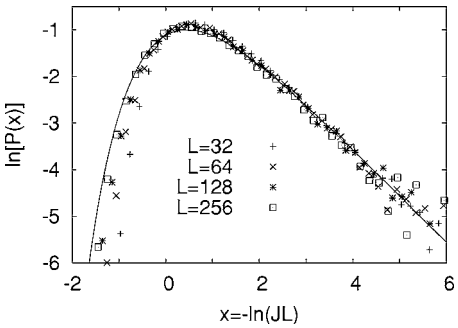

FIG. 3. The distribution of the current, calculated with uniform randomness with $q_0=1/3$, where $z=1.335$. The number of samples is 10 000. The solid line is the Fréchet distribution given in Eq. (16).

$$P(\tilde{J}) = \frac{2}{z}\tilde{J}^{2/z-1}e^{-\tilde{J}^{2/z}}, \tag{16}$$

in terms of $\tilde{J}=J_0JL^{z/2}$, where the nonuniversal constant J_0 depends on the prefactor of the tail. Thus, the current scales with the system size as given in Eq. (15).

Although the above results hold for generic hop rate distributions, a caveat is in order concerning the type of randomness. Besides the bimodal one, one may also consider hop rate distributions where the support of the forward rates p does not have a positive lower bound, such as for the power-law distribution in Eq. (7). In this case it may happen that the current is limited by the lowest hop rate $p_{min} \sim L^{-D}$—i.e., by a single slow link rather than by the maximal amplitude of a Brownian excursion, which is given in Eq. (15). Clearly, the exponent which enters in Eq. (16) and as well as in the scaling relation of the current (15) is now $\max\{z/2, D\}$. For a uniform distribution with $D=1$ the current scales as $J(L) \sim L^{-z/2}$ for $z>2$ whereas $J(L) \sim L^{-1}$ for $1<z<2$. Numerical results for the distribution of current in the anomalous region $1<z<2$ are shown in Fig. 3, whereas numerical results for the bimodal randomness, for which the anomalous scenario never sets in, can be found in Ref. [12]. In what follows we assume that $z/2>D$ always holds and the current is controlled by an extended region.

2. Density profile

The density profile for general form of disorder has the same qualitative features as for the extreme disorder in Sec. IV A. The system consists of a high-density phase, where all the lattice sites are typically occupied, and of a low-density phase, in which all the lattice sites are typically vacant. The front separating the two phases is just at the middle of the largest barrier (see Fig. 4). In the low-density phase only the large valleys with $U_l \geqslant U_m/2$ are filled to a level $U_l - U_m/2$. Similarly, in the high-density phase only the large barriers with $U_l \geqslant U_m/2$ are partially filled up to $U_m/2$.

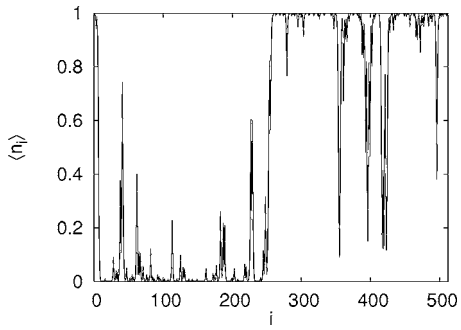

FIG. 4. Numerically calculated stationary density profile of a sample of size $L=512$. The hop rates were generated with the bimodal distribution with $c=0.3$ and $r=0.5$ in Eq. (5).

The number of occupied valleys, $n(L)$ (and the number of partially filled barriers), can be estimated from the condition that at these barriers the single-particle trapping time be larger than $1/J$; thus,

$$n(L) \sim L \int_{1/J}^{\infty} p(\tau) d\tau \sim L J^{1/z}, \tag{17}$$

where we used (11) and the fact that, due to their finite typical extension, the number of barriers in the system is of the order of L. Keeping in mind the scaling relation of the current in (15), we obtain $n(L) \sim L^{1/2}$, in agreement with the extreme disorder case in Sec. IV A. This finding is in good agreement with numerical results shown in Fig. 5.

The length of Brownian excursions has an exponential distribution [35], with a finite Δ-dependent characteristic value. Although the length of the $L^{1/2}$ longest excursions is $O(\ln L)$ [23], the length of the empty domain in each of these barriers equals approximately half of the length of the largest barrier, so one can show that the number of particles they contain is typically finite.

The total number of particles clustering behind the subleading barriers is thus of the order of $L^{1/2}$. The other $O(L)$ particles must be behind the largest barrier, where a macroscopic cluster of particles is formed. According to the discussion given above, the particles can be categorized into three classes as was carried out in a similar way for the disordered zero-range process [12].

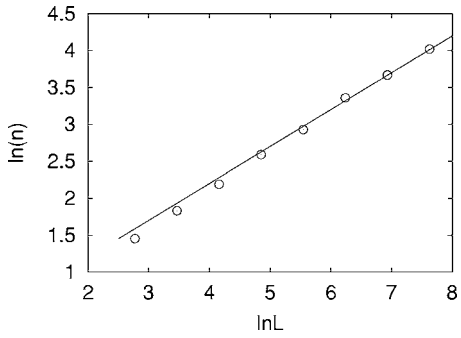

FIG. 5. Average number of points where the density profile crosses the line $\rho(x)=1/2$ calculated numerically for different system sizes L. Binary randomness were used with $r=0.5$ and $c=0.2$, whereas the average was performed over 100 samples. The straight line has slope of 1/2.

Almost all particles are trapped at the largest barrier, forming a *condensate*, where the density is close to 1. The spatial extension of the condensate, which is equal to the number of trapped particles, is thus

$$N_c \sim N. \tag{18}$$

This region is, however, cut into sections of size $\sim L^{1/2}$ by vacant clusters, which have a finite length.

In the remaining part of the system which is of size $\sim(L-N)$, particle clusters of finite size are found, separated by a typical distance of $L^{1/2}$. Due to the small local velocity in these dense clusters, the contribution of a single particle to the current is small compared to freely moving particles; therefore, we call these particles *inactive*. Their total number is given by

$$N_{ia} \sim L^{1/2}. \tag{19}$$

The third class of particles, the *active* ones, move practically freely between clusters of inactive particles. Consequently, they have a significant contribution to the current. In order to estimate the number of active particles, we notice that due to the low particle density within sections between two neighboring clusters of inactive particles the dynamics of active particles corresponds to the dynamics of a single random walker in a disordered landscape. The typical length of these section is $\sim L^{1/2}$, and the largest trapping time of an active particle is $\sim\sqrt{\tau_1} \sim L^{z/2}$. Now, if $z<1$, the particle velocity v is L independent. Making use of the finite-size scaling form of the current, we obtain for the density $\rho=J/v \sim L^{-z/2}$, which is indeed vanishing in the large-L limit. The total number of active particles is thus

$$N_a \sim L^{1-z/2} \quad (z<1). \tag{20}$$

For $z>1$, the largest barrier in the empty section determines the travel time and the average velocity of particles scales according to $v(L) \sim L^{(1-z)/2}$. The density thus scales as $\rho=J/v \sim L^{-1/2}$, which means that typically $O(1)$ particles reside between two inactive clusters. In this case the total number of active particles is given by

$$N_a \sim L^{1/2} \quad (z>1). \tag{21}$$

According to the discussion above, the distribution of interparticle distances in a finite system of size L has a finite cutoff: they have the scaling form $\bar{l} \sim L^{z/2}$ for $z<1$, whereas $\bar{l} \sim L^{1/2}$ for $z>1$.

Next, the number of particles at the second largest barrier n_2 is analyzed. The height of the second largest barrier is proportional to $\ln L$ just as the height of the largest one. For the bimodal randomness where the increments of the potential are fixed, the length of the barrier must grow with the system size at least as $O(\ln L)$. On the other hand, it is generally true for types of randomness under consideration, where the current is controlled by an extended cluster of exponentially rare links. The typical value for $\langle n_2 \rangle$ is thus $O(\ln L)$. In certain samples, however, where the single-

particle trapping times τ_1 and τ_2 at the first and second largest barriers, respectively, are almost degenerate, meaning that $\tau_2 \lesssim \tau_1$, the occupation $\langle n_2 \rangle$ is much larger than the typical value $O(\ln L)$. We show below that these samples give a singular contribution to the sample-averaged occupation $[\langle n_2 \rangle]_{av}$. In samples where the two largest barriers are almost degenerate, n_2 has large-scale fluctuations and the dominant contribution to the thermal average $\langle n_2 \rangle$ comes from the fluctuations where n_2 is much larger than its most probable value. In the latter case half-filling is realized at the second barrier, leading to an escape time $\sqrt{\tau_2}$. Not considering the improbable samples with higher degeneracies (the contribution of which has in fact the same type of singularity), the number of particles located at barriers other than the two largest ones is negligible and the problem reduces to an effective two-barrier process with hop rates $\sqrt{\tau_1}$ and $\sqrt{\tau_2}$. Taking into account, that the total number of particles is N, we obtain for the thermal average [12]

$$\langle n_2 \rangle(\alpha) = \frac{\alpha}{1-\alpha} - (N+1)\frac{\alpha^{N+1}}{1-\alpha^{N+1}}, \quad \alpha < 1, \tag{22}$$

where $\alpha \equiv \sqrt{\tau_2/\tau_1}$ and $\langle n_2 \rangle = N/2$ for $\alpha = 1$. Using the distribution function $\rho(\alpha)$, we can average over realizations: $[\langle n_2 \rangle]_{\mathrm{av}} = \int_0^1 \langle n \rangle(\alpha)\rho(\alpha)\mathrm{d}\alpha$, which is dominated by the contribution as $\alpha \to 1$, where $\rho(\alpha)$ has a finite limiting value. Keeping in mind that the maximal value of $\langle n_2 \rangle$ is $N/2$, we can write

$$[\langle n_2 \rangle]_{\mathrm{av}} \approx \int_0^{1-2/N} \frac{\alpha}{1-\alpha}\rho(\alpha)\mathrm{d}\alpha \sim \rho(1)\ln N. \tag{23}$$

Thus the rare samples, where the second largest trapping time can be arbitrarily close to the largest one, give a logarithmically diverging contribution to the sample-averaged occupation at the second barrier.

C. Low-density limit

Contrary to the previous section, where the global density $\rho = N/L$ was finite, we study here the case where the number of particles scales as $N \sim CL^a$ for large L, with $0 \leqslant a < 1$. This implies that the particle density is vanishing algebraically according to $\rho(L) \sim CL^{a-1}$ as $L \to \infty$. In this case the number of active particles may be limited by N, which influences the current.

We have learned in the previous section, that the system has a limited capacity for storing particles, given by $N_a + N_{ia}$, and the excess of particles is driven to the macroscopic condensate. Evidently, as long as N exceeds the capacity of the system, $N_a + N_{ia}$, the excess particles accumulate in the condensate and the largest barrier is half filled. Consequently the current remains the same as the one observed for constant density. This is, however, no longer true if N is smaller then the capacity of the system.

For $z > 1$, the capacity scales as $(N_a + N_{ia}) \sim L^{1/2}$ according to (21) and (19). Thus, for $a > 1/2$, the current and the number of active and inactive particles are not influenced, whereas $N_c \sim L^a$. However, if $a < 1/2$, the condensate vanishes, and since one can show that N_a is proportional to N_{ia} for arbitrary current, both must be proportional to L^a. Therefore according to (17) the current is given by $J \sim [n(L)/L]^z \sim L^{-z(1-a)}$.

For $z < 1$, the capacity is dominated by N_a, which scales according to (20). Thus, as far as $a > 1 - z/2$, the number of active and inactive particles and the current agrees with the case of a finite density, whereas the size of the condensate scales as $N_c \sim L^a$. If $a < 1 - z/2$, there is no condensate present in the system and the number of active particles is limited to $N_a \sim L^a$. Therefore the corresponding current scales as $J \sim L^{-(1-a)}$. Then the number of inactive particles scales as $N_{ia} \sim n(L) \sim L^{1-(1-a)/z}$ according to Eq. (17), which is indeed a vanishing fraction of the active particles, which we have tacitly assumed. According to the latter expression, if $z + a < 1$, $N_{ia} \to 0$ as $L \to \infty$, meaning that all particles are active.

Setting $a = 0$ in the scaling forms obtained for the current we recover the exact results known for the Sinai walk.

V. ZERO AVERAGE BIAS

If the control parameter is zero, $\Delta = 0$, the average tilt of the potential landscape and, consequently, the sample-averaged current are zero even for finite systems. However, as a consequence of the fluctuations of randomness, the potential landscape of a single sample of size L is tilted, having a typical slope of $L^{-1/2}$, in accordance with central-limit theorem. Therefore the quantity of interest is the magnitude of the current for a finite system.

As the symmetric point is approached, $\Delta \to 0$, both the typical length and amplitude of Brownian excursions are diverging as $\xi \sim \Delta^{-2}$ and $U_m \sim \Delta^{-1}$, respectively. According to the central-limit theorem the typical amplitude is then of the order of $L^{1/2}$; consequently, the magnitude of the current vanishes rapidly with the system size as

$$-\ln|J| \sim L^{1/2}. \tag{24}$$

Since the largest excursion covers an $O(1)$ fraction of the landscape, its internal structure has to be investigated in order to get some insight into the properties of the density profile. We consider first a finite sample with $\Delta_L \equiv \sum_{i=1}^{L}(\ln p_i - \ln q_i) = 0$, where the potential is single-valued and the current is zero. In the stationary state of this sample the particles practically occupy the N lowest-potential sites and the clusters of occupied sites are represented by Brownian excursions. (These are not to be confused with barriers, which are excursions starting at extremal sites of the landscape.) The number of such excursions, n, in a system of size L is estimated as follows. For $\Delta = 0$, the asymptotic distribution of their length is

$$p_l \sim l^{-3/2}; \tag{25}$$

thus, the length of the largest one among n excursions, l_{max}, is typically of the order n^2. On the other hand, n is related to L via $n\int_1^{l_{max}} l p_l dl \sim L$, yielding $n \sim L^{1/2}$ and $l_{max} \sim L$. Thus, the potential landscape contains $O(L^{1/2})$ excursions and the largest one of them is macroscopic. If the landscape is tilted, but

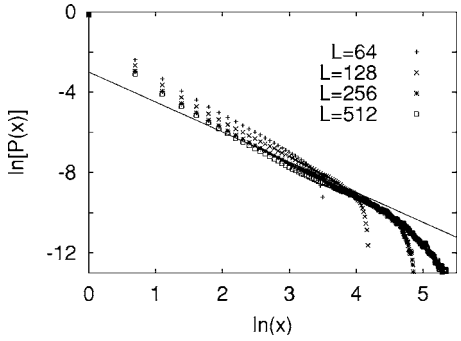

FIG. 6. Distribution of interparticle distances calculated numerically with the bimodal distribution with $c=0.5$ and $r=0.2$. The number of samples is 5000. The slope of the straight line is $-3/2$.

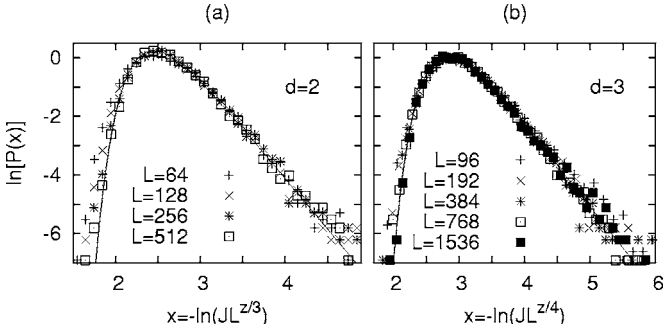

FIG. 7. Distribution of the current for the exclusion process with particles of size $d=2$ (a) and $d=3$ (b), computed for different system sizes. The number of particles is $N=L/(2d)$. Bimodal randomness was used with $c=0.2$, $r=0.3$, where $z=0.869$ (a), and $c=0.3$, $r=0.3$, where $z=1.420$ (b), whereas the number of samples is 10^4. The solid curves are the Fréchet distributions given in Eq. (16).

L is large, one can still construct an approximate profile by cutting the landscape by a straight line, the slope of which corresponds to the tilt of the landscape. Then sites below the line are filled with particles. Since the current as well as the typical tilt of samples vanishes as $L\to\infty$, the profile constructed in this way is expected to be not much different from the true stationary profile.

According to the above one expects that the distribution of interparticle distances has the asymptotics as given in (25), with a finite cutoff $O(L)$. Indeed, numerical results are in satisfactory agreement with these predictions; see Fig. 6.

VI. RELATED MODELS

In this section we shall apply the phenomenological description developed above to two generalizations of the disordered exclusion process.

A. Particles of size d

First, we consider a process, where the particles occupy $d\geqslant 1$ subsequent lattice sites whereas they take steps of unit length as before [36]. Obviously, the single-particle trapping time at a certain barrier, τ, is not influenced by d. However, the time scale for holes to overcome the same barrier which is now filled by particles of size d is reduced to $O(\tau^{1/d})$, since the holes take steps of length d; consequently, the effective potential barrier they have to overcome is reduced by a factor of d. Thus, particle-hole symmetry is broken for $d>1$ and half-filling at the largest barrier does not hold anymore. Instead, the largest barrier is filled with particles up to some level $\frac{b-1}{b}\tilde{U}_m$ where the parameter b is to be determined from the equality of particle current and hole current, reading as $e^{-\tilde{U}_m(b-1)/(bd)}=de^{-\tilde{U}_m/b}$. For large $\tilde{U}_m$ this yields $b=1+d$; consequently, the current scales as

$$J\sim L^{-z/(1+d)}, \tag{26}$$

where we made use of the scaling relation $e^{\tilde{U}_m}\sim L^z$. Following the arguments of the previous section, similar results can be derived here, as well. For instance, the current follows a Fréchet distribution (see Fig. 7 for numerical results) and the number of inactive particles scales with the system size L as

$$N_{ia}\sim L^{d/(1+d)}. \tag{27}$$

Finally, we mention that the model with $d=2$ is related to a PASEP in which the particles are linked, meaning that the number of empty sites between two neighboring particles can be at most 1. It is easy to see that the motion of holes in this model follows the same rules as, say, the left half of $d=2$ particles in the original model. In biological transport systems, molecular motors are often attached to a rigid backbone, where the distance between motors is limited to a finite value [37]. Exclusion processes with linked particles may be relevant for modeling the cooperative behavior in these type of systems.

B. Exclusion process with multiple occupation

Our second example is the disordered version of the generalized exclusion process [38], where the number of particles at a given site is limited by the site-independent integer $K\geqslant 1$. The topmost particles at a given site jumps to one of the neighboring sites with site-dependent rates p_i and q_i, provided that the occupation at the target site is smaller than K. This model evidently interpolates between the exclusion process ($K=1$) and the zero-range process ($K=N$). Moreover, it can be roughly interpreted as an exclusion process where the size of particles, $d\equiv 1/K$, is smaller than 1.

In the stationary state of this generalized model we still expect a front at the largest barrier separating an almost fully occupied region (with K particles per site) from an almost empty region. Moreover, particle-hole symmetry holds for $K>1$, as well; therefore, half-filling must be realized at the largest barrier and the current scales with the system size for any finite K as for $K=1$. Numerical results for the distribution of the current are presented in Fig. 8.

One can also consider the L dependence in K, such as $K=K_0L^k$, with $0<k<1$, leading to a scaling of the number of inactive particles according to $N_{ia}\sim KL^{1/2}\sim L^{1/2+k}$. The results of the previous section concerning the low-density limit can be generalized for this case in a straightforward way.

We mention, finally, that regarding the number of particles at a given site as a distance variable, the present model

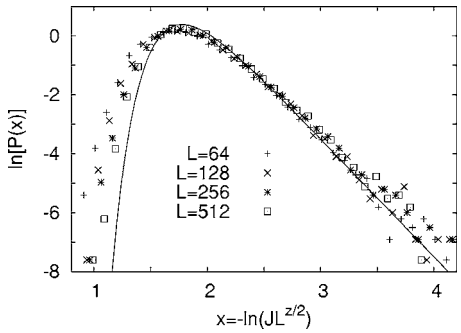

FIG. 8. Numerically calculated distributions of the current for the generalized exclusion process with $K=4$, for different system sizes. The number of particles is $N=KL/2$. Bimodal randomness was used with $c=0.2$ and $r=0.5$, where $z=0.5$, whereas the number of samples is 10^4. The solid curve is the Fréchet distribution given in Eq. (16).

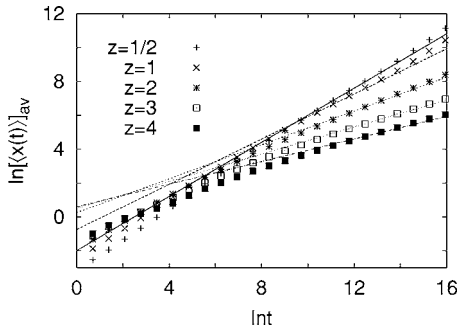

FIG. 9. Time dependence of the average displacement of a single particle measured for different values of $\Delta \neq 0$. Bimodal randomness was used with $c=\frac{1}{3}$ and $r=\frac{1}{\sqrt{2}}, \frac{1}{2}, \frac{1}{4}, \frac{1}{8}, \frac{1}{16}$ where $z=\frac{1}{2}, 1, 2, 3, 4$, respectively. The size of the system is $L=8192$ whereas $N=4096$ and the disorder average was performed over 200 samples. The straight lines have the slope $\frac{2}{z+2}$ for each z.

can be mapped to an exclusion process with particlewise disorder, for any K, where the distance between neighboring particles can be at most K.

VII. NONSTATIONARY PHENOMENA

A. Coarsening

In the following we analyze the approach to the stationary state in an infinite system. When the system is started in a homogeneous configuration, it undergoes a coarsening process in the course of which the typical size of high-density and low-density regions, $l(t)$, is growing [6]. The growth rate of these regions is determined by the current leading to the differential equation

$$\frac{dl(t)}{dt} \sim |J(l(t))|, \tag{28}$$

where the current $J(l(t))$ is a function of the time-dependent length scale. By making use of the scaling relation of the current (15) which is valid for $\Delta \neq 0$ we get for large t

$$l(t) \sim t^{1/\zeta}, \quad \zeta = \frac{z}{2} + 1 \quad (\Delta \neq 0), \tag{29}$$

where ζ is the dynamical exponent related to the coarsening. We mention that the same scaling relation has already been derived for the bimodal distribution, with z' instead of z [6], which is therefore valid only in the $c \to 0$ limit. Using (28) and (29), the asymptotic time dependence of the current is given by

$$J(t) \sim t^{-z/(2+z)} \quad (\Delta \neq 0). \tag{30}$$

When the symmetric point is approached—i.e., $\Delta \to 0$—the exponent z given in Eq. (12), and consequently the dynamical exponent ζ diverges as $\zeta \sim z \sim 1/(2\Delta)$ [28]. Thus, strictly at the symmetric point $\Delta=0$, the length scale is growing slower than any power of t, a phenomenon called anomalous coarsening. Substituting the scaling relation of the current (24) into (28), we get the asymptotic solution $l^{1/2} e^{Cl^{1/2}} \approx t$, leading to

$$l(t) \sim \left[\ln\left(\frac{t}{\ln t} \right) \right]^2 \quad (\Delta = 0), \tag{31}$$

which is indeed an anomalously (logarithmically) slow growth. Using (28) we obtain for the asymptotic time dependence of the magnitude of the current

$$|J(t)| \sim \frac{\ln t}{t} \quad (\Delta = 0). \tag{32}$$

It is, however, circumstantial to measure the size of dense regions in numerical simulations since they are not connected. Instead, we considered the average displacement of particles $\langle x(t) \rangle$ as a function of time for $\Delta \neq 0$, which is related to the current according to $\frac{d\langle d(t) \rangle}{dt} = \frac{1}{\rho} J(t)$. Comparing this relation with (28) we see that $\langle x(t) \rangle$ grows in time as the length scale $l(t)$. Results of numerical simulations shown in Fig. 9 are in good agreement with the phenomenological predictions.

We mention that the cutoff of the interparticle distance distribution $\bar{l}(t)$ is growing slower than $l(t)$. If $z<1$, the interparticle distances in the low-density regions of size $l(t)$ are proportional to $[l(t)]^{z/2}$ and thus grow as $\bar{l}(t) \sim t^{z/(2+z)}$. If $1<z<\infty$, the interparticle distances in the low-density regions are proportional to $[l(t)]^{1/2}$, leading to $\bar{l}(t) \sim t^{1/(2+z)}$.

B. Invasion

We consider in this section an open semi-infinite lattice with entrance rate $\alpha=1$; furthermore, it is assumed that the lattice is initially empty. Our interest is in the invading dynamics—i.e., the dynamics of the first particle that enters the system and the motion of the bulk of particles. This question is of practical relevance; e.g., one may think of a fluid penetrating a porous medium.

First, we study how the position of the leading particle evolves in time. Apparently, it must not travel slower than a single walker since the jumps to the right are never hindered, contrary to jumps to the left. Thus, for $z<1$ the first particle advances with a constant velocity. For $z>1$, we consider a

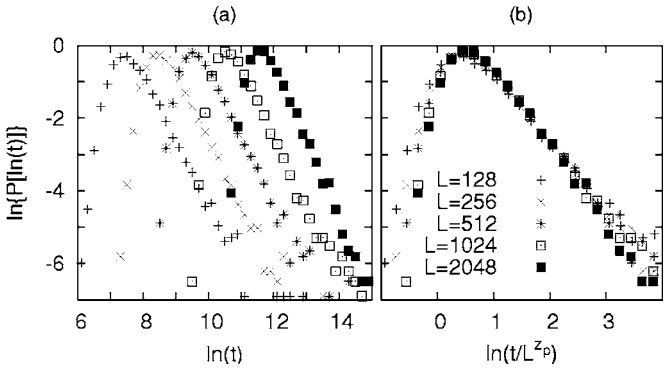

FIG. 10. Distribution of invasion times calculated for different system sizes. Bimodal randomness was used with $c=0.3$ and $r=0.2$, where $z_p \approx 1.45$. The number of samples is 10^4.

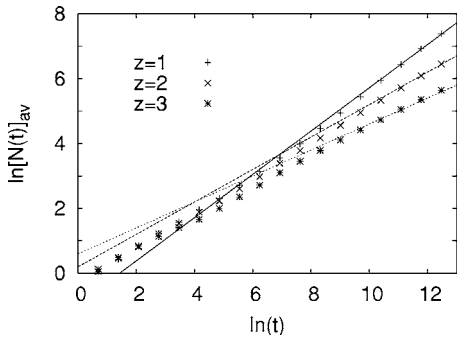

FIG. 11. Time dependence of the average number of particles of measured for different values of $\Delta \neq 0$. Bimodal randomness was used with $c=\frac{1}{3}$ and $r=\frac{1}{2},\frac{1}{4},\frac{1}{8}$ where $z=1,2,3$, respectively. The size of the system is $L=8192$, and the disorder average was performed over 200 samples. The straight lines have the slope $\frac{2}{z+2}$ for each z.

finite system of size L and determine the finite-size scaling of the characteristic time τ_p needed for the first particle to reach site L, as follows. The leading contribution to τ_p comes from the trapping time at the largest barrier and at subsequent barriers. Therefore we assume that the first particle has already arrived at the largest barrier of the system. Without the other particles, the typical time to overcome the barrier would be $\tau_1 \sim L^z$. However, during this period other particles are arriving at the barrier with rate $O(L^{-z/2})$ determined by the current at the half-filled largest barrier between the entrance site and leading particle. The size of the largest barrier is at most $\sim \ln L$, so it takes at most a period of $t \sim L^{z/2} \ln L$ until half-filling of the largest barrier is achieved. Once half-filling is realized, the trapping time for the leading particle is only $O(L^{z/2})$, so the total trapping time at the largest barrier is at most $O(L^{z/2} \ln L)$.

After leaving the largest barrier, the first particle advances freely until it arrives at a barrier with trapping time larger than $\sqrt{\tau_1}$, where it is assisted in passing the barrier again by other particles. The typical time scale to fill the barrier is determined by the current and therefore given by $t \sim L^{z/2}$. Using the assistance of the following particles the trapping time of the first particle at the barrier is given by $O(L^{z/2})$. Since there are $O(L^{1/2})$ barriers with trapping time $\tau > \sqrt{\tau_1}$ in a sample of size L, the characteristic time for getting through the system scales in leading order as $\tau_p \sim L^{z/2+1/2}$. Therefore in a semi-infinite system, the position of the leading particle ξ_p is expected to scale as

$$\xi_p \sim t^{1/z_p}, \quad \text{with } z_p = \frac{z+1}{2}, \tag{33}$$

for $z > 1$, whereas $z_p = 1$ for $z < 1$.

In order to test the validity of our approach, we have checked the above results numerically by measuring the distribution of times the first particle needs to traverse a finite system. The results are in good agreement with the scaling relation (33), as shown in Fig. 10. For zero average bias, the exponent z_p is formally infinite and the propagation of the first particle is anomalously slow.

Compared to the first particle, the bulk of particles moves slower, as we shall show below. For large times, $t \gg 1$, a dense particle cluster is present in the system, which extends from the entrance site to a barrier which is located at $\xi_f(t)$ and which must be the largest barrier of the interval $[0, \xi_f(t)]$. Since this barrier is half-filled, the current it maintains is typically of the order of $\xi_f(t)^{-z/2}$. Through this (source) barrier, particles are constantly moving to the next larger barrier to its right. The escape rate at this second barrier is typically $[2\xi_f(t)]^{-z/2}$, which is a finite fraction of the filling current; therefore, the domain behind it is being filled up by particles with a rate $\sim J \sim \xi_f(t)^{-z/2}$. (Those particles which escape at the second barrier meanwhile, rush forward, to the third and subsequent larger barriers spreading in the domain behind the leading particle.) After a certain time the domain between the source and the second barrier is completely filled and the new position of the front is now at the second barrier. Thus the growth rate of the dense cluster is proportional to the current, $\frac{d\xi_f(t)}{dt} \sim J \sim \xi_f(t)^{-z/2}$, yielding that the typical position of the front scales with the time as

$$\xi_f(t) \sim t^{1/\zeta}, \tag{34}$$

with a larger dynamical exponent than that of the leading particle. In order to check this numerically we have measured the number of particles, $N(t)$, as a function of time, which is expected to grow as ξ_f. Results of numerical simulations, shown in Fig. 11, are in good agreement with (34).

VIII. DISCUSSION

In this paper we have studied the partially asymmetric exclusion process with lattice disorder and we have obtained several conjecturedly exact results both for the stationary state and for related nonstationary problems. In particular for the biased system we have shown a phase separation phenomenon where a domain wall taking place in the middle of the largest barrier separates a low- and a high-density phase. The stationary current in a large finite system goes to zero as a power law, and the corresponding exponent is just the half of the dynamical exponent of a single random walker. We have also classified the particles, which typically belong to a macroscopic condensate. This condensate, however, is cut up

by $O(L^{1/2})$ vacant regions of finite size, which are located at the subleading barriers of the potential landscape. These vacant regions, through the particle-hole symmetry, correspond to filled deep valleys in the low-density phase, which contain the so-called inactive particles. Finally, the third type of particles are the active ones, which actually carry the current in the system. We have also studied the properties of the system in nonstationary processes, such as coarsening or invasion, and have shown that the scaling exponents are related to the dynamical exponent of a single random walker.

Comparing the effect of different types of disorder on the stationary behavior of the PASEP we can notice some analogies but also several differences. For both particle and lattice disorder the stationary current is vanishing as a power law of the size of the lattice and the critical exponents are connected via a simple relation. Also the phase-separation phenomenon is common for the two problems. The system with particle disorder can be treated by renormalizing the particles [11], arriving at an effective model containing only a single particle. Renormalization for lattice disorder has only been performed for a single particle [32], leading to a motion of the particle in a renormalized landscape. For many particles it is expected that both the landscape and the particles should be renormalized and the resulting model is still a many-particle problem. The actual construction of the renormalization procedure is the purpose of future research.

ACKNOWLEDGMENTS

R.J. and L.S. acknowledge support by the Deutsche Forschungsgemeinschaft under Grant No. SA864/2-2. This work has been supported by the National Office of Research and Technology under Grant No. ASEP1111, by a German-Hungarian exchange program (DAAD-MÖB), by the Hungarian National Research Fund under Grants Nos. OTKA TO37323, TO48721, K62588, MO45596, and M36803. F.I. is grateful to C. Monthus for valuable discussions.

[1] B. Schmittman and R. K. P. Zia, *Statistical Mechanics of Driven Diffusive Systems* (Academic Press, London, 1995).
[2] G. M. Schütz, in *Phase Transitions and Critical Phenomena*, editel by C. Domb and J. L. Lebowitz (Academic Press, San Diego, 2001), Vol. 19.
[3] D. Chowdury, L. Santen, and A. Schadschneider, Phys. Rep. **329**, 199 (2000).
[4] C. Bustamante, Y. R. Chemla, N. R. Forde, and D. Izhaky, Annu. Rev. Biochem. **73**, 705 (2004).
[5] S. A. Janowsky and J. L. Lebowitz, Phys. Rev. A **45**, 618 (1992); J. Stat. Phys. **77**, 35 (1994).
[6] J. Krug, Braz. J. Phys. **30**, 97 (2000).
[7] M. Barma, Physica A **372**, 22 (2006) (special issue).
[8] T. Chou and G. Lakatos, Phys. Rev. Lett. **93**, 198101 (2004).
[9] G. Lakatos, J. O'Brien, and T. Chou, J. Phys. A **39**, 2253 (2006).
[10] G. Tripathy and M. Barma, Phys. Rev. Lett. **78**, 3039 (1997); Phys. Rev. E **58**, 1911 (1998).
[11] R. Juhász, L. Santen, and F. Iglói, Phys. Rev. Lett. **94**, 010601 (2005).
[12] R. Juhász, L. Santen, and F. Iglói, Phys. Rev. E **72**, 046129 (2005).
[13] For a review see J. P. Bouchaud and A. Georges, Phys. Rep. **195**, 127 (1990).
[14] For a review see F. Iglói and C. Monthus, Phys. Rep. **412**, 277 (2005).
[15] D. S. Fisher, Phys. Rev. Lett. **69**, 534 (1992); Phys. Rev. B **51**, 6411 (1995).
[16] D. S. Fisher, Phys. Rev. B **50**, 3799 (1995).
[17] J. Hooyberghs, F. Iglói, and C. Vanderzande, Phys. Rev. Lett. **90**, 100601 (2003); Phys. Rev. E **69**, 066140 (2004).
[18] U. Gerland, R. Bundschuh, and T. Hwa, Phys. Biol. **1**, 19 (2004).
[19] M. R. Evans, Europhys. Lett. **36**, 13 (1996).
[20] M. R. Evans, T. Hanney, and Y. Kafri, Phys. Rev. E **70**, 066124 (2004).
[21] C. Enaud and B. Derrida, Europhys. Lett. **66**, 83 (2004).
[22] R. J. Harris and R. B. Stinchcombe, Phys. Rev. E **70**, 016108(E) (2004).
[23] J. Galambos, *The Asymptotic Theory of Extreme Order Statistics* (John Wiley and Sons, New York, 1978).
[24] R. Juhász, Y.-C. Lin, and F. Iglói, Phys. Rev. B **73** 224206 (2006).
[25] L.-H. Gwa and H. Spohn, Phys. Rev. Lett. **68**, 725 (1992); Phys. Rev. A **46**, 844 (1992).
[26] For a review see R. B. Stinchcombe, Adv. Phys. **50**, 431 (2001).
[27] B. Derrida, J. Stat. Phys. **31**, 433 (1983).
[28] F. Iglói and H. Rieger, Phys. Rev. E **58**, 4238 (1998).
[29] S. Redner, *A Guide to First-passage Process* (Cambridge University Press, Cambridge, England, 2001).
[30] P. Lévy, *Processus Stochastiques et Mouvement Brownien* (Gauthier-Villars, Paris, 1965).
[31] H. Kesten, Acta Math. **131**, 298 (1973); B. Derrida and H. Hilhorst, J. Phys. A **16**, 2641 (1983); C. de Calan, J. M. Luck, T. M. Nieuwenhuizen, and D. Petritis, *ibid.* **18**, 501 (1985).
[32] P. Le Doussal, C. Monthus, and D. S. Fisher, Phys. Rev. E **59**, 4795 (1999).
[33] C. Monthus, Phys. Rev. E **67**, 046109 (2003).
[34] R. A. Blythe *et al.*, J. Phys. A **33**, 2313 (2000).
[35] F. Iglói and H. Rieger, Phys. Rev. B **57**, 11404 (1998).
[36] L. B. Shaw, J. P. Sethna, and K. H. Lee, Phys. Rev. E **70**, 021901 (2004).
[37] J. Howard, *Mechanics of Motor Proteins and the Cytoskeleton* (Sinauer, Sunderland, 2001).
[38] C. Kipnis and C. Landim, *Scaling Limits of Interacting Particle Systems* (Springer, Berlin, 1999).